Aerosol Optical/Radiative Forcing Properties over East Asia Determined from SKYNET Radiation Measurements

B.J. Sohn[1], Do-Hyeong Kim[1], Teruyuki Nakajima[2], and Tamio Takamura[3]

School of Earth and Environmental Sciences, Seoul National University, Seoul, Korea[1]
Center for Climate System Research, University of Tokyo, Tokyo, Japan[2]
Center for Environmental Remote Sensing, Chiba University, Chiba, Japan[3]
E-mail: Sohn@snu.ac.kr

Abstract

We developed a method of retrieving aerosol optical properties and their associated radiative forcing from simultaneously measured sky radiation and surface solar flux data. The method is then applied to data sets collected at Mandalgovi, Dunhuang, Yinchuan, and Sri-Samrong sites of the Skyradiometer Network (SKYNET), and at Anmyon, Gosan, and Amami-Oshima, to examine the aerosol characteristics of East Asia. From the analysis for the SKYNET sites, it was found that aerosols in East Asia have smaller single scattering albedos (i.e., 0.89 for Asian dusts in Dunhuang, 0.9 for urban type aerosols in Yinchuan, and 0.88 for biomass burning aerosols in Sri-Samrong), compared to the single scattering albedo for the same type of aerosols found in other areas. Lower single scattering albedo suggests that the aerosols over East Asia absorb comparatively more solar radiation. The measurements taken during April at the latter three sites over the Korean peninsula, and the East China Sea showed that the single scattering albedo of Asian dust becomes smaller during the course of its movement from the source region to East Asian sea waters (i.e., 0.86 at Anmyon, 0.84 at Gosan, and 0.80 in Amami-Oshima), compared with 0.89 found in the source region (i.e., Dunhuang). These findings strongly suggest that Asian dusts become blackened during the movement because of mixing with soot particles produced over the industrial/urban area of China. The overall atmospheric forcing efficiency (radiation flux per unit aerosol optical thickness at 0.5 μm) of Asian dusts ranges from 65 W m^{-2} to 94 W m^{-2} near the East Asian seaboard area, indicating that atmospheric heating by Asian dusts can be significantly enhanced by the mixing with soot particles.

Keyword: aerosol, East Asia, solar radiation, aerosol radiative forcing .

1. Introduction

In East Asia, in order to determine the physical, chemical, and radiative properties of aerosols, as well as to quantify aerosols-radiation interactions, the Asian-Pacific Regional Aerosol Characterization Experiment (ACE-Asia) was conducted over the East China Sea (Huebert et al., 2003). The physical and chemical processes controlling the evolution of the major aerosols were also studied. The results of ACE-Asia have shown that dusts in Asia can be transported half way around the globe, and air pollution can significantly change dust aerosols by adding black carbon, toxic materials, and acidic gases to the mineral particles (Huebert et al., 2003). It was also found that a 24 hour-averaged clear-sky shortwave net radiative forcing ranges from -26 ~ -30 W m^{-2} over East Asian oceanic and coastal region (Markowicz et al., 2003; Bush and Valero, 2003)

Despite the importance of the Asian continent as an aerosol source region there have been few measurements, especially in the desert area of north China. Moreover, due to the large spatiotemporal variations of aerosols, long-term monitoring near the source regions or their downwind areas is needed. Focusing on long-term monitoring of aerosols and an assessment of aerosol impact on the climate system over East Asia, a ground-based aerosol/radiation observation network, named the Skyradiometer Network (SKYNET), has been operating since 1997. Instruments used for observing surface solar radiation and aerosol characteristics include skyradiometer, pyranometer, and pyrheliometer. In addition, due to the interest in dust impact on the local and global climate, field experiments were conducted over East Asian seawaters, i.e., the Asian Atmospheric Particle Environmental Change Studies (APEX) (Nakajima et al., 2003).

In this study, we will investigate the magnitude and varying degrees of aerosol influence on the solar radiation budget at the surface and TOA over East Asia using surface solar radiation measurements taken at SKYNET sites. Effort will also be made to interpret the relationship of these measurements to retrieved aerosol optical parameters. To this end, we developed a method of estimating ARF using retrieved aerosol optical parameters from skyradiometer measurements. In doing so, adjusted imaginary parts of refractive indices (and then single scattering albedos) estimated from the diffuse/direct method, originally introduced by King and Herman (1979) and extended by Nakajima et al. (1996), were used as inputs into the exact radiative transfer (RT) model instead of using direct retrievals from skyradiometer measurements. In addition, special measurements taken during April in Korea and Japan were also analyzed in order to investigate the influences of Asian dust on radiative forcing downwind of East Asia.

2. Observation and analysis

Direct and diffuse solar radiation were measured using a sky radiometer (POM-01L, Prede Co. Ltd.) in daytime at seven wavelengths of 315, 400, 500, 675, 870, 940, and 1020 nm. Aerosol optical thickness, single-scattering albedo at five wavelengths (400, 500, 675, 870, and 1020 nm), Ångström exponent, and

volume size distribution [$dV/d\ln r$ (cm^3cm^{-2})] were retrieved using an inversion software (i.e.: SKYRAD.pack version 3) developed by Nakajima et al. (1996). A detailed explanation about quality control, retrieval methods, and sensitivity analysis can be found in Kim (2003), and Kim et al. (2004).

For the radiative forcing calculation, surface solar radiation measurements in the wavelength band between 0.3 and 4.0 μm were used in conjunction with aerosol optical properties obtained from the skyradiometer measurements. Direct solar fluxes were measured by the pyrheliometer, which measures the intensity of a radiant beam at normal incidence coming only from the solar disk with about 5 degrees of the full opening view angle. A shaded pyranometer was used to measure diffuse solar radiation, as both the pyranometer and the shading disk were mounted on an automated solar tracker to ensure that the pyranometer was continuously shaded. Then global downwelling solar fluxes were determined from direct solar radiation measured by pyrheliometer multiplied by the cosine of the solar zenith angle plus diffuse radiation by the shaded pyranometer. Although global downward solar fluxes were also measured by the pyranometer, the pyranometer tends to be more uncertain when the solar zenith angle is high because the detector responds differently to the solar incident angle (Michalsky et al., 1995; Satheesh et al., 1999). Thus, the global fluxes determined from both pyrheliometer and shaded pyranometer were preferable to those measured by the pyranometer.

Measurements were taken at seven sites, given in Figure 1. Among them, four observation sites, i.e., Mandalgovi, Dunhuang, Yinchuan, and Sri-Samrong, form the SKYNET, while the Anmyon, Gosan sites of Korea, and the Amami-Oshima site of Japan are for the special radiation measurements made during the spring.

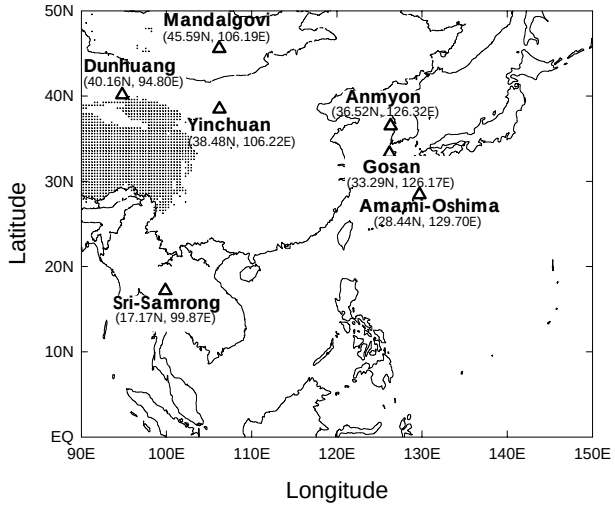

Figure 1: Geographical locations of observation sites.

3. Methodology for radiative forcing calculation

For the radiative forcing calculation, we have developed an algorithm, adjusting aerosol parameters to bring in calculated values of diffuse and direct solar radiation close to observed values. Retrieval procedures used for the calculation of aerosol radiative forcing from ground-based solar radiation measurements are provided in Figure 2. As illustrated at the top of Figure 2, aerosol optical parameters and atmospheric profiles are used as inputs into a RT model for simulating surface solar fluxes. For the flux calculation, we use the real part of refractive index retrieved from sky radiance measurements. Thus values vary with space and time, ranging from 1.45 to 1.70. During the retrieval, the columnar water vapor amount and the imaginary part of the refractive index (hereafter absorption index) are obtained by minimizing the difference between the calculated and measured fluxes, as suggested in King and Herman (1979), and Nakajima et al. (1996). In doing so, the absolute accuracies of the pyrheliometer and pyranometer are used as the convergence criteria (ε) in Figure 2. The adjusted absorption index and columnar water vapor amount are then used for the forcing calculation.

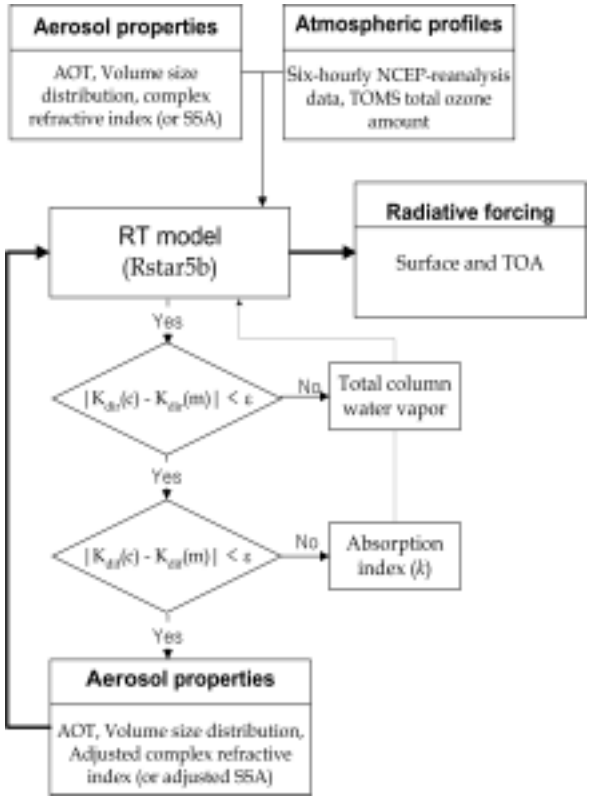

Figure 2: A schematic diagram for the procedures used in aerosol radiative forcing calculation from skyradiometer and surface solar flux measurements. K_{dir} and K_{dif} represent direct and diffuse fluxes, *c* and *m* in parentheses represent calculated and measured values, respectively.

4. Aerosol Radiative Forcing over East Asia

For an ARF calculation, simultaneous measurements of sky radiation and diffuse/direct solar radiation flux at the surface are required. Because of limited match-ups of sky radiation vs. solar flux data due to the inhomogeneous data coverage, the ARF coverage is also limited. Therefore, ARF is given with the number of match-ups used for the forcing calculation in each month—see the left panels of Figure 3. The

middle panels of Figure 3 display the 24-hour averaged surface ARFs (W m^{-2}) given with AOT at 0.5 μm at Dunhuang, Yinchuan, and Sri-Samrong. The match-ups available for Mandalgovi were not enough to represent aerosol forcing characteristics in that area, so that results obtained from measurements for Mandalgovi are not presented.

The relatively small number of available data for each month was largely due to the cloud contamination. However, it was also contributed by the employed assumption that the SSA from sky radiation measurents should be consistent with the adjusted SSA, allowing only a small adjustment to satisfy the measured surface radiation fluxes. The retrieved SSA from the flux method was compared against the one from sky radiation measurements only, and then the retrieval was discarded if the difference was greater than 0.05. In Figure 3, calculated ARFs (represented by cross hairs) are given as a function of optical thickness at 0.5 μm. Also provided are theoretically calculated SSAs (represented by curves) at 0.5 μm, which range from 1.0 (top curve) to 0.6 (bottom curve) with a 0.05 interval. For the simpler demonstration using the reduced number of parameters, theoretical SSAs at each site were calculated using mean values of aerosol volume size distribution and surface albedo, but with varied optical thickness. Because of this, some points appear to have unrealistic SSAs greater than unity. Also given in the middle panels of Figure 3 are the mean SSA and *g*. In addition, mean β at the TOA, atmosphere, and surface are provided in the right panels of Figure 3.

As expected Dunhuang is influenced mainly by dust particles all year around. In Yinchuan, the general aerosol characteristics are related to the accumulation processes of urban aerosols throughout the year, and dusts during the springtime. Sri-Samrong showed patterns for biomass burning aerosols during mid-October to mid-February. The results obtained in this study over those three sites will be interpreted with the aid of typical aerosol types found at those observation sites. Details of aerosol characterization and their seasonal variations for those sites are found in Kim et al. (2004).

Because Dunhuang is largely affected by frequent Asian dust episodes during the spring to early summer period, ARFs for Dunhuang found in this study are largely due to Asian dust aerosols. The mean SSA and *g* are 0.89 and 0.71, respectively. The SSA obtained in this study at 0.5 μm is slightly smaller than 0.92~0.93 at 0.44 μm found over the Saharan desert or Saudi Arabia (Dubovik et al., 2002a), implying that Asian dusts are more absorbing aerosol. On the other hand, the obtained *g* (≈0.71) is close to the values found in the Saharan desert (≈0.72) or Saudi Arabia desert (≈0.68) (Dubovik et al., 2002a).

The resultant forcing efficiency in the atmosphere is about 67 W m^{-2}, suggesting that Asian dusts over the Dunhuang area absorb a significant amount of solar radiation. Combining with the relatively smaller forcing efficiency at the TOA (≈-9 W m^{-2}), the overall surface forcing efficiency is estimated to be -76 W m^{-2}, indicating that the surface is deprived of a substantial amount of solar energy in the presence of Asian dusts. The smaller TOA forcing efficiency seems to be associated with high surface reflectivity over the Dunhuang area, since the negative TOA forcing can be reduced by the aerosol absorption of surface-reflected upwelling radiation, in particular under high surface albedo conditions, as noted in Sahara dust studies (Haywood et al., 2001; Haywood et al., 2003; and Myhre et al., 2003). More discussion on the influences of Asian dusts on the ARF is found in Kim et al. (2004).

Yinchuan represents the urban type aerosol because the match-up data only cover the September-December period. The obtained SSA of around 0.9 is similar to the SSA (0.87 to 0.90) found over the Indian Ocean during the INDOEX period (Satheesh and Ramanathan, 2000). However, 0.9 of SSA in Yinchuan is much smaller than 0.98 at 0.44 μm for urban type aerosols observed at the NASA Goddard Space Flight Center (GSFC) (Dubovik et al., 2002a). This variability of SSA for urban type aerosols may be due to differences in fuel types and emission conditions. Automobile traffic should be the main local source of the pollution around the GSFC. On the other hand, the highly absorbing optical properties in the INDOEX are mainly due to the presence of soot type aerosols from inefficient fossil fuel combustion for heating and cooking, and biomass burning (Satheesh et al., 1999). Considering that aerosols from inefficient fossil fuel combustion are also abundant over China (Chameides et al., 1999), we suspect that the small SSA value in Yinchuan is also due to the contributions of soot type aerosols to SSA.

The period from December to March corresponds to the dry winter season over the Sri-Samrong area, and thus the prevailing aerosol type is the biomass burning (Kim et al., 2004). The retrieved SSA (≈0.88) representing biomass burning aerosols over the Sri-Samrong area is slightly larger than the 0.85 for African Savanna smoke but smaller than the 0.93 for the smoke over Amazonian forested regions (Eck et al., 1998; Eck et al., 2001; Dubovik et al., 2002). There are two bundles of points separated by about 0.9 line of SSA; one showing the mean SSA around 0.91 during December 1998 and the other showing a smaller mean SSA around 0.86 during January to March in 1998. The different SSAs suggest that aerosol origin and composition during December are different from those for the January-March period, i.e., there are more absorbing aerosols during the latter period.

Acknowledgements: This research has been supported by ADD/KAIST of Korea, and also by the APEX Project of the Japan Science and Technology Corporation.

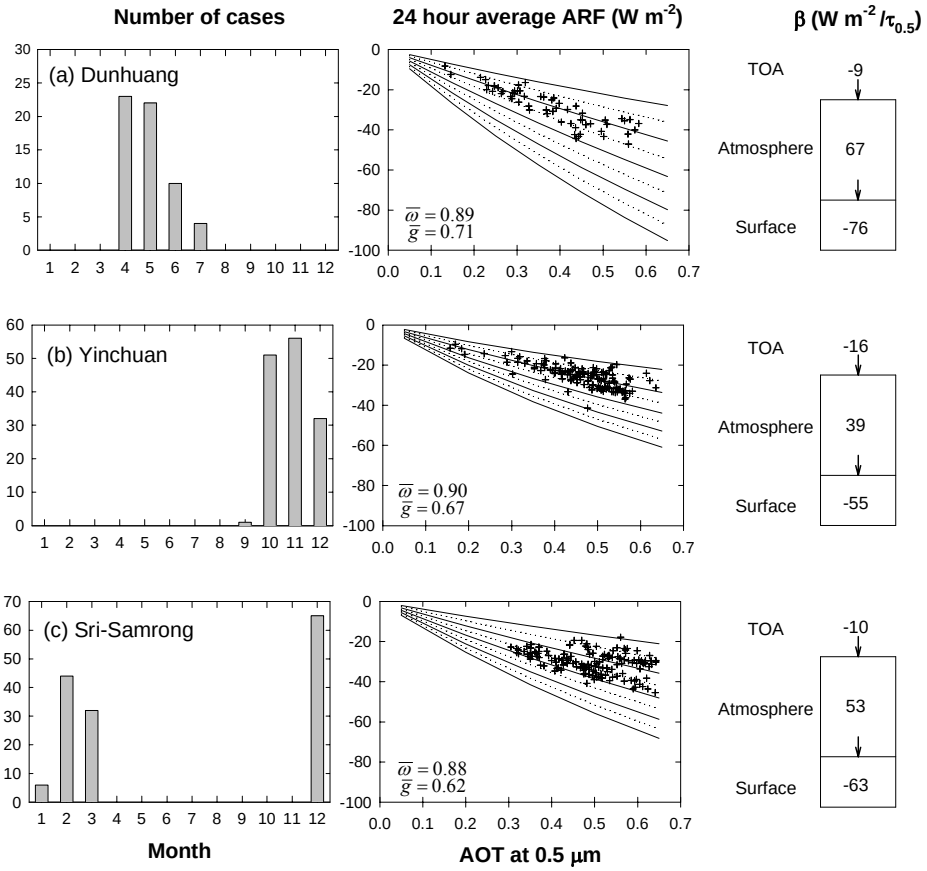

Figure 3: Number of cases used in each month (left), 24-hour averaged surface radiative forcing (W m^{-2}) with AOT at 0.5 μm (middle), and forcing efficiency (β) given in W m^{-2} (right) at Dunhuang (top), Yinchuan (middle), and Sri-Samrong (bottom). Curves represent the theoretical radiative forcing calculated with SSAs of 1.0 (top) to 0.6 (bottom), with a 0.05 interval. Cross hairs represent observed forcing. $\overline{\omega}$ and $\overline{g}$ represent mean single scattering albedo and asymmetry factor at 0.5 μm, respectively.

References

Dubovik, O., A. Smirnov, B. N. Holben, M. D. King, Y. J. Kaufman, T. F. Eck, and I. Slutsker, Accuracy assessment of aerosol optical properties retrieved from Aerosol Robostic Network (AERONET) sun and sky radiance measurements, *J. Geophys. Res., 105*, 9791-9806, 2000.

Eck, T. F., B. N. Holben, I. Slutsker, and A. Setzer, Measurements of irradiance attenuation and estimation of aerosol single scattering albedo for biomass burning aerosols in Amazonia, *J. Geophys. Res.*, *103,* 31,865-31,878, 1998.

Kim, D. H., B. J. Sohn, T. Nakajima, T. Takamura, T. Takemura, B. C. Choi, and S. C. Yoon, Aerosol optical properties over East Asia determined from ground-based sky radiation measurements, *J. Geophys. Res. 109*, D02209, doi:10.1029/2003JD003387, 2004.

King, M. D., and B. M. Herman, Determination of the ground albedo and the index of absorption of atmospheric particulates by remote sensing. Part I: Theory, *J. Atmos. Sci.*, *36*, 163-173, 1979.

Nakajima, T., and M. Tanaka, Matrix formulations for the transfer of solar radiation in a plane-parallel scattering atmosphere, *J. Quant. Spectrosc. Radiat. Transfer, 35*, 13-21, 1986.

Nakajima, T., T. Hayasaka, A. Higurashi, G. Hashida, N. Moharram-Nejad, Y. Najafi, and H. Valavi, Aerosol optical properties in the Iranian region obtained by ground-based solar radiation measurements in the summer of 1991, *J. Appl. Meteor., 35*, 1265-1278, 1996b.

Ramanathan, V., and Co-authors, Indian Ocean Experiment: An integrated analysis of the climate forcing and effects of the great Indo-Asian haze, *J. Geophys. Res*., *106,* 28,371-28,398, 2001b.

Sugimoto, N., A. Shimizu, and I. Matsui, Observations of aerosols and clouds with lidars, *Fifth APEX International Workshop*, Miyazaki, Japan, 3-5 June 2002, 2002.

Tanre, D., Y. J. Kaufman, B. N. Holben, B. Chatenet, A. Karnieli, F. Lavenu, L. Blarel, O. Dubovik, L. A. Remer, and A. Sminov, Climatology of dust aerosol size distribution and optical properties derived from remotely sensed data in the solar spectrum, *J. Geophys. Res*., *106,* 18,205-18,217, 2001.